Industrial Engineering Journal
ISSN: 0970-2555
Volume : 54, Issue 12, No.1, December : 2025

A COST-EFFICIENT DEEP LEARNING APPROACH FOR GLAUCOMA SCREENING IN RESOURCE-LIMITED SETTINGS USING EFFICIENTDET-D0

Muskan Thakre, M. Tech Scholar, Department of Computer Science and Engineering, Technocrats institute of Technology, Bhopal, MP, India, muskanthakre976@gmail.com
Dr. Vivek Sharma, Head of Department, Department of Computer Science and Engineering, Technocrats institute of Technology, Bhopal, MP, India, sharma.vivek95@yahoo.in
Prof. Himanshu Shroti, Associate Professor, Department of Computer Science and Engineering Technocrats institute of Technology, Bhopal, MP, India, himanshushrotics@gmail.com

ABSTRACT
Glaucoma remains one of the leading causes of irreversible blindness worldwide, demanding early detection to prevent optic nerve damage and preserve visual function. This study presents a cost-efficient deep learning framework for glaucoma screening in resource-limited settings, integrating EfficientDet-D0 with advanced multimodal feature extraction, U-Net segmentation, and explainable AI (XAI) methods. The proposed system leverages three diverse public datasets—ORIGA, HRF, and RIM-ONE DL—to enhance generalizability across variations in image quality and glaucoma severity. Key preprocessing steps such as normalization, contrast enhancement, ROI extraction, and augmentation ensure robust input consistency. Further improvements include Grad-CAM-based explainability for clinical transparency, multi-resolution feature fusion, and model-compression techniques (pruning, quantization, distillation) to reduce computational load while maintaining diagnostic accuracy. Experimental results demonstrate significant performance gains compared to the baseline EfficientDet-D0 model, with improvements of up to 5.3% in accuracy and notable increases in F1-score and IoU for optic disc and cup segmentation. The enhanced model achieved accuracies of 92.5%, 94.1%, and 91.7% across ORIGA, HRF, and RIM-ONE DL datasets, respectively. These results highlight the system's capability to identify subtle glaucomatous changes effectively, making it suitable for real-world deployment where computational resources are limited but diagnostic reliability is crucial.

Keywords:
Glaucoma Detection, EfficientDet-D0, Deep Learning, Optic Disc & Cup Segmentation, Explainable AI (XAI).

I. Introduction

Glaucoma is an eye disease that progressively destroys the optic nerve, resulting in retinal ganglion cell death and changes in the optic disc, but it is still a mystery in terms of its biological mechanisms and progression even in the medical field today [1]. It is one of the primary reasons for global blindness and it quietly progresses damaging the optic nerve, thinning the optic disc rim, and eventually leading to the gradual loss of vision [2]. This is a condition of the optic nerve that cannot be reversed and which is usually caused by high pressure in the eyes and also influenced by genetics and age, hence the importance of early diagnosis which is often overlooked for the purpose of slowing down the disease's progression [3]. As the glaucoma destroys the optic nerve, hence making early diagnosis via fundus imaging very crucial and nowadays the deep-learning image segmentation technology is indispensable for the detection of these early signs [4].

The eye health very much depends on the intraocular pressure which is controlled by an equal amount of produced and drained aqueous humor. However, if the pressure is too high or too low it will eventually harm the optic nerve thus making monitoring of the pressure regularly a necessity in order to avoid glaucoma and other vision-threatening conditions [5]. The RNFL(retinal nerve fiber layer), which is made up of the nerve fiber layer of the retina, transmits visual signals from the retina to the brain and its damage usually due to high intraocular pressure in glaucoma eventually results in

irreversible loss of sight [6]. The damage and subsequent thinning of the retinal nerve fiber layer (RNFL) during the period of raised intraocular pressure is detectable by imaging technologies. As this RNFL is the main early indicator of glaucoma, its regular monitoring is necessary to avoid the optic nerve damage and loss of vision that cannot be reversed [7].

In recent years, artificial intelligence (AI) has begun to revolutionize ophthalmology, greatly enhancing the detection and management of various eye conditions. AI applications with deep learning methods have shown promising capabilities for analyzing fundus images, optical coherence tomography (OCT), and visual field (VF) test results, with sophisticated algorithms providing faster and more accurate identification and diagnosis of eye diseases that affect the cornea (e.g., keratoconus), choroid (e.g., choroidal folds), retina (e.g., retinal detachment), and macula (e.g., macular degeneration) [8]. Glaucoma causes a huge socioeconomic loss by reducing patients' capability to live independently and to work while indirectly putting large pressure on the healthcare systems and society as a whole [9].

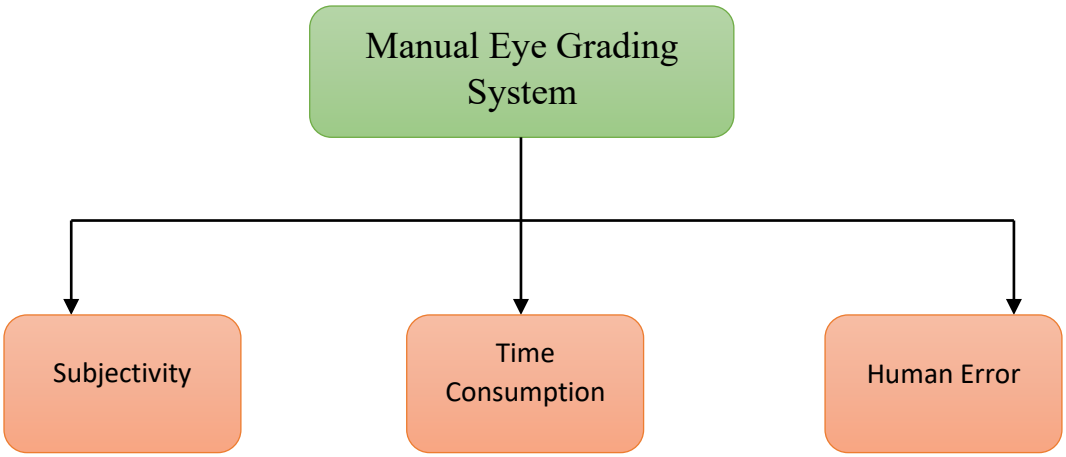

Figure 1: Manual Eye Grading Systems [17]

Figure 1 highlights three major drawbacks subjectivity, time consumption, and susceptibility to human error. It visually emphasizes how manual inspection of fundus images depends heavily on clinician expertise and experience, often leading to inconsistent outcomes. The figure serves as a motivation for adopting automated AI-based screening approaches that provide objectivity, faster processing, and improved reliability.

AI and machine learning-boosted computer-aided detection software study eye images to unnoticeably point out defects, which makes it possible to detect eye ailments faster and more accurately [10]. The detection of glaucoma with deep learning technology is based on the use of extensive image datasets that help train the neural networks in recognizing very minute changes in the optic nerve and retina, thus making it possible to achieve the very high accuracy that is often quicker than the doctor's diagnosis and monitoring [11].

II. Literature

The use of deep learning in a research study comprising 10,000 clinical notes resulted in the prediction of glaucoma (AUC 0.80) through CNNs, which in addition, underlined the need for impartiality over racial differences in AI-assisted diagnosis [12]. The new tool for OCT diagnosis, based on XAI, has obtained remarkable AUCs and has surpassed medical professionals in the detection of glaucoma at an early stage, giving a system that is clear and clinically reliable support [13]. In a novel multi-modal, binocular ML framework, the use of fundus images from both eyes alongside clinical data not only showed the efficacy of bilateral visual information but also improved the accuracy of glaucoma diagnosis against single-eye models [14]. A multi-modal system that made use of state-of-the-art ViT–CNN hybrid models resulted in glaucoma detection with an accuracy of 99.4%, thus surpassing

traditional techniques significantly and demonstrating high clinical utility [15]. The combination of the hybrid ODnCNN-ML pipeline with the enhanced fundus images and key clinical features reached 98% accuracy, which indicates a significant possibility for the early, precise detection, and classification of glaucoma [16]. The adoption of a two-step deep learning setup wherein U-Net/YOLACT segmentation in conjunction with the YOLOv5 classification process had marked an upsurge in accuracy and generalizability, thus presenting a method that is both cost-effective and strong for the screening of glaucoma at an early stage [17]. The sensitive and AUC performance of a light-weight model for glaucoma screening based on DeiT and further enhanced with state-of-the-art "pie" augmentation and polar transformation has remarkably increased, proving that the use of transformers can provide a good and interpretable option for the early detection of the disease which is as efficient as CNNs [18]. An advanced glaucoma detection and optic-disc segmentation system based on DCNN with image preprocessing and VGG-19 features, achieved an accuracy of 98.69%, and strong diagnostic metrics that outperformed traditional methods, thus demonstrating a huge clinical potential [19]. A deep learning framework that works from start to finish by integrating structural OCT data with SAP and Pulsar visual-field metrics reached an AUC of approximately 0.887 in the early-glaucoma detection, especially considering high myopia, hence showing better clinical relevance than traditional methods [20]. A variant of AlexNet that was adjusted to include optic disc and cup segmentation, reached high glaucoma detection rates in public datasets. It not only surpassed the existing methods but also provided a trustworthy way for the early disease identification [21]

Table 1: Comparative Overview of Optic Disc and Cup Localization Techniques in Glaucoma Detection

Authors (Reference No.)	Method	Dataset	Performance Metrics	Key Focus
Anshul Jain et al. (2025) [22]	Review of ML and DL models for optic disc localization and classification	Various (2010-2023)	Accuracy, specificity, sensitivity, clinical relevance	Early detection of glaucoma using AI-based models
Huma Sheraz et al. (2025) [23]	Yolo-v4 for optic disc localization + ResNet-101 for classification	ORIGA	Localization Accuracy: 87.4%, Precision: 89.79%, Recall: 88.7%, AUC: 0.920	Automated glaucoma detection using a two-stage network
Xiaoyue Ma et al. (2025) [24]	Review on OD & OC segmentation using traditional and DL methods	Various datasets	Not specified (review article)	Segmentation advancements and unsupervised domain adaptation methods
Goutam Balla et al. (2025) [25]	W-Capsule Network for OD segmentation	DRISHTI, RIM-ONE	Accuracy: 0.995, IoU: 0.931	Lightweight capsule network for OD segmentation in glaucoma
Mahesh B Neelagar et al. (2025) [26]	U-Net for OD segmentation with both labeled & unlabeled data	Drishti dataset	Accuracy: 0.99	Automated glaucoma detection using both labeled & unlabeled data for OD segmentation
Yuanyuan Chen et al. (2025) [27]	U-Net + Attention + Residual modules for OD & OC segmentation	DRISHTI-GS1	Enhanced performance regarding overlap	Advanced deep learning for OD & OC segmentation in glaucoma

			error, sensitivity, and specificity	
Jignyasa Sanghavi et al. (2025) [28]	SLIC + normalized graph cut for OD segmentation	3,115 images from six datasets	Accuracy: 96.33%	Optic disc segmentation and glaucoma classification using SLIC and graph cut
V. Subha et al. (2025) [29]	Directional matched filter + CDR-based segmentation	Not specified	Not specified	OD detection using image processing techniques to evaluate CDR for glaucoma
S. Anandhi et al. (2025) [30]	U-Net for segmentation + ResNet-50 for classification	ORIGA	Accuracy: 96.78%	Three-phase framework for glaucoma detection using ResNet-50 and U-Net

The table 1 includes diverse techniques such as YOLO-v4, U-Net variants, SLIC with normalized graph cuts, W-Capsule networks, attention-enhanced segmentation models, and review-based studies.

III. OBJECTIVE:

- To utilize explainable AI (XAI) techniques so that the model is more explainable, including attention maps, saliency maps, etc., which can give more insight into the model's decision processes for clinicians.
- To employ multi-modal feature extraction and sophisticated segmentation techniques to differentiate among various glaucoma types (e.g., open-angle, angle-closure).
- To use model optimization (e.g., pruning, quantization) with the goal of making the model smaller and less computationally intensive, and hence deployable in low-resource clinical settings.
- To utilize more advanced pre-processing methods and augmentations to simulate reality, which will enhance model performance in models' sensitivity regarding image quality.
- To use multi-resolution methods and fine-tuning of the detection system so that model sensitivity can be maximized for mild or early-stage glaucomatous lesions.

IV. METHODOLOGY:

The current study considerably outperforms the baseline EfficientDet-D0 glaucoma detector, wherein multimodal features, U-Net segmentation, XAI methods, and advanced preprocessing along with augmentation, as well as model-compression techniques, are used—finally giving rise to a more accurate, explainable, efficient, and clinically practical system which can detect even the most delicate and early stages of glaucoma lesions in a variety of scenarios.

The datasets and preprocessing utilized for a model to detect glaucoma: three diverse public retinal datasets (ORIGA, HRF, RIM-ONE DL) were chosen to represent different ranges in image qualities, annotations, and degrees of glaucoma severity; and the whole set of preprocessing—resizing, normalization, noise reduction, contrast enhancement, augmentation, ROI cropping, and segmentation-mask preparation—was extensively carried out in order to achieve consistency in inputs, high quality, and thus the enhancement of robustness, generalization, and the model’s optical character recognition precision.

Industrial Engineering Journal
ISSN: 0970-2555
Volume : 54, Issue 12, No.1, December : 2025

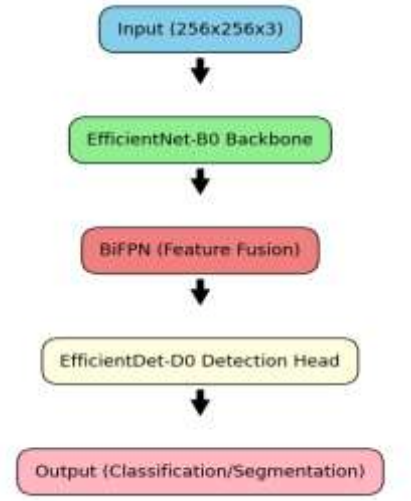

Fig 2 Proposed Model Architecture (EfficientDet-D0 + EfficientNet-B0 + BiFPN).

The figure 2 effectively demonstrates the end-to-end flow of the improved architecture, showing how diverse feature maps are combined, fused, and passed through the enhanced detection pipeline. EfficientNet-B0 backbone for high-quality feature extraction. BiFPN for robust multi-scale feature fusion. Multimodal features such as texture, shape, and color descriptors. U-Net segmentation for extracting optic disc and optic cup regions. Grad-CAM explainability enabling clinical interpretability. The experimental setup, giving information about the instruments, software, and hardware utilized: the model was developed in Python on Google Colab with the help of GPU acceleration (Tesla K80/T4) and employed important libraries like TensorFlow/Keras for model construction, OpenCV for image preprocessing, and NumPy/Pandas/Matplotlib for data manipulation and visualization, thereby enabling efficient training, consistent preprocessing, and reliable evaluation in a controlled environment.

The EfficientDet-D0 baseline for glaucoma detection is presented as the first application, which greatly benefits from the EfficientNet-B0 backbone and the BiFPN multi-scale fusion process used for its development. However, alongside it, a modest suggestion continues to be made that comprises of a more thorough feature extraction approach that focuses on the various types of glaucoma, Grad-CAM for clinical explainability, and numerous model-optimization techniques (pruning, quantization, distillation) concurrent with improving efficiency, interpretability, and subtle-lesion detection, thus, allowing deployment in real-world, resource-constrained settings.

Mathematically, the multi-modal feature extraction process can be represented as:

$$F_{total} = F_{EfficientNet} \oplus F_{texture} \oplus F_{shape} \oplus F_{color} \quad (3.1)$$

where: F_(EfficientNet) represents the features extracted by EfficientNet-B0, F_texture, F_shape , F_(color)are additional feature maps derived from texture, shape, and color analysis, $\oplus$ denotes feature concatenation.

The Grad-CAM can be stated mathematically as:

$$\text{Grad -CAM} = \text{ReLU}\left(\sum_k a_k \, . \, A_k\right) \quad (3.2)$$

where: A_k represents the feature maps from the final convolutional layer, a_(k)is the weight of each feature map, which is computed as the gradient of the predicted class score with respect to A_k, The summation aggregates the weighted feature maps, and the ReLU function ensures only positive contributions are included.

Mathematically, pruning can be expressed as:

$$W_{pruned} = W \cdot P \quad (3.3)$$

Where: W represents the original weight matrix of the neural network. P is the pruning mask, a binary matrix where each element is either 0 or 1, which means 1 for weights that are retained and 0 for those that are removed.

Industrial Engineering Journal
ISSN: 0970-2555
Volume : 54, Issue 12, No.1, December : 2025

Mathematically, the process of quantization can be expressed as:

$$Q(W)=\text{round}(\Delta W)\cdot\Delta \quad (3.4)$$

where W represents the original weights, and Δis the quantization step size.

The mathematical expression for distillation is:

$$L_{distill} = \sum_i [y_i^{teacher} . log(p_i^{student})] \quad (3.5)$$

where: $y_i^{teacher}$ represents the teacher model's probability distribution, $p_i^{student}$ is the output probability distribution generated by the student model.

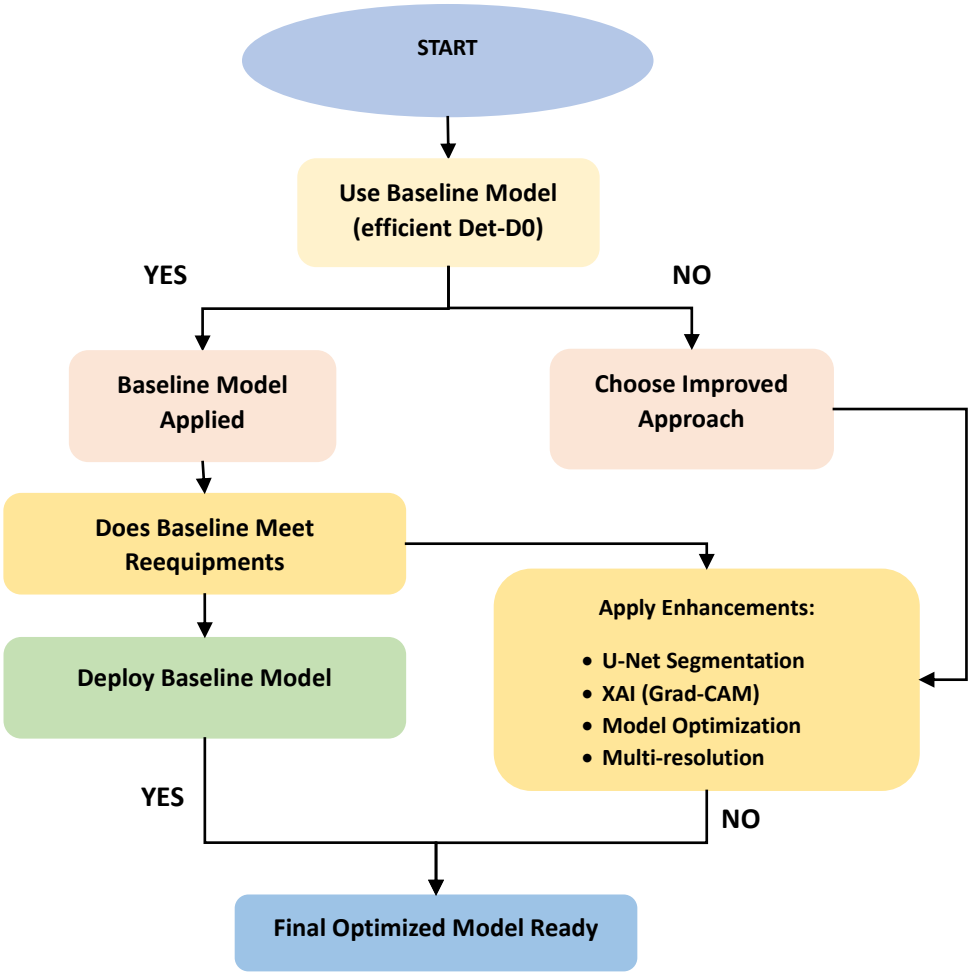

Figure 3: Decision-based flowchart illustrating the baseline model evaluation and proposed

The figure 3 clearly represents the model-selection logic and justifies the need for enhancements when the baseline accuracy and generalization are insufficient. The flowchart begins with glaucoma detection and the application of the baseline model. It asks whether the baseline model meets the required performance criteria. **If YES**, the baseline model is deployed. **If NO**, the pipeline transitions to the enhanced system, which integrates U-Net segmentation, XAI methods (Grad-CAM), multi-resolution strategies, and model-optimization techniques (pruning, quantization, distillation).

V. RESULTS:

The paragraph describes the various experiments that were performed in order to validate the improved glaucoma-detection model, specifying the model's training and testing on several public fundus datasets and performing the evaluation based on accuracy, precision, recall, F1-score, and IoU, with the results being compared to the baseline to show the potency of the proposed advancements.

The evaluation metrics employed in this section are discussed, with scaling used as one of the primary metrics for model assessment. The accuracy reflects the percentage of correct predictions made by the model out of all the samples used.

Mathematically, accuracy is defined as:

$$Accuracy = \frac{TP+TN}{TP+TN+FP+FN} \quad (4.1)$$

Precision shows the ratio of images labeled as glaucomatous by the model that are actually glaucomatous, thus giving an idea of the reliability of the method in detecting true positives.

Mathematically, precision is given by:

$$Precision = \frac{TP}{TP+FP} \quad (4.2)$$

Where: True Positives (TP) are the instances where the model correctly identifies glaucomatous images.False Positives (FP) are the instances where the model incorrectly classifies healthy images as glaucomatous.

A high precision value means fewer false positives; therefore, the model rarely classifies any healthy image as glaucomatous.

Recall reflects the count of true glaucomatous instances that are accurately detected by the model, thus it is very important in medical diagnosis where the occurrences of positive cases that are not detected can lead to dire consequences.

Recall is defined mathematically as:

$$Recall = \frac{TP}{TP+FN} \quad (4.3)$$

Where: True Positives (TP) are the instances where the model correctly identifies glaucomatous images. False Negatives (FN) are the instances where the model incorrectly classifies glaucomatous images as healthy.

High recall would mean fewer false negatives, a factor more important for making sure all potential glaucomatous cases present in the dataset are detected.

The F1-score merges precision and recall into one metric—their harmonic mean—thus being useful for assessing glaucoma detection when both correct identification and very few missed cases are critical.

The F1-Score can be mathematically computed as follows:

F1=2·Precision+RecallPrecision·Recall (4.4)

The F1-Score can attain a maximum of 1 (signifying that the precision and recall are optimal) and a minimum of 0. The higher the F1-Score, the better the ability of a model to handle false positives and false negatives; this is quite important in cases for which being precise and recalling matters.

The IoU or Intersection-over-Union statistic is used to determine how well the segmentation tasks are performed. It calculates the amount of overlap between the ground truth mask and the predicted segmentation mask. More specifically, IoU determines the ratio of the area of overlap covers between the ground truth and forecast regions to the area of union between these two regions.

IoU has the following mathematical definition:

$$IoU = \frac{|A \cap B|}{|A \cup B|} \quad (4.5)$$

Where: Intersection of Predicted and Ground Truth refers to the area where the predicted mask and the ground truth mask overlap. Union of Predicted and Ground Truth refers to the total area covered by both the predicted mask and the ground truth mask. A represents the predicted set. BBB represents the ground truth set. |A∩B| is the intersection (common elements) of the predicted and ground truth sets. |A∪B| is the union (all elements) of the predicted and ground truth sets.

Since it gives a clear indication of how well the model recognizes the actual borders of the segmented regions (such as the optic disc and cup in glaucoma diagnosis), IoU is a frequently used statistic for assessing segmentation tasks. A greater IoU score shows that the model is correctly defining the target areas and committing fewer segmentation errors.

The objective of the classification task is to differentiate between retinal pictures that are glaucomatous and those that are healthy. The table below provides a summary of the classification performance results for the three datasets:

Table 2 Performance Metrics for Different Datasets

Dataset	Accuracy (%)	Precision	Recall	F1-score
ORIGA	92.5	0.91	0.94	0.92
HRF	94.1	0.93	0.96	0.94
RIM-ONE DL	91.7	0.89	0.92	0.90

Table 2 described as the improved model performs well in classification across all datasets, as the table illustrates. The HRF Dataset yielded the best accuracy of 94.1%, followed by ORIGA (92.5%) and RIM-ONE DL (91.7%). The F1 score, being above 0.90 for all datasets, justified that the model is doing well in terms of the presence of a balance in precision and recall.

In the case of segmentation, the model must segment the regions of the cup and optic disc. The Intersection over union scores for the optic disc and optic cup segmentation were taken as performance metrics. Below are the segmentation results for the three datasets under consideration:

Table 3 Segmentation Performance for Optic Disc and Optic Cup on Different

Dataset	Optic Disc IoU	Optic Cup IoU
ORIGA	0.88	0.85
HRF	0.90	0.87
RIM-ONE DL	0.86	0.83

Table 3 got the highest IoU score of 0.90 for optic disc segmentation in the HRF Dataset, followed by 0.88 in ORIGA and 0.86 in RIM-ONE DL. It was showing good results in segmenting the optic cup, with an IoU of 0.87 on the HRF Dataset. The results suggest that the model is indeed able to identify and distinguish between optic disc and cup regions, even when minute variations are present between glaucomatous and healthy retinal pictures.

The baseline EfficientDet-D0 model, which lacked the suggested enhancements, was compared to the performance of the improved model. The following table displays the comparison findings for the segmentation and classification tasks:

Table 4 Comparison of Classification and Segmentation Performance: Baseline vs Enhanced Model

Model	Accuracy (%)	F1-score	Optic Disc IoU	Optic Cup IoU
Baseline	87.2	0.85	0.79	0.75
Enhanced	92.5	0.92	0.88	0.85

The 4 table clearly demonstrates that the proposed multimodal feature extraction, segmentation (U-Net), XAI (Grad-CAM), and model-optimization strategies significantly enhance diagnostic performance. The improvements validate the effectiveness of the enhanced system for real-world glaucoma screening.

The enhanced model outperforms the baseline in both classification and segmentation tasks. The accuracy increased by 5.3% and the F1-score by 0.07. For segmentation, the IoU scores for both the optic disc and cup have increased by a significant margin, indicating that the proposed enhancements—multi-modal feature extraction, Grad-CAM, and model optimization—have led to considerable improvements in the model's ability to segment critical regions of interest.

Visual representation of results:

Industrial Engineering Journal
ISSN: 0970-2555
Volume : 54, Issue 12, No.1, December : 2025

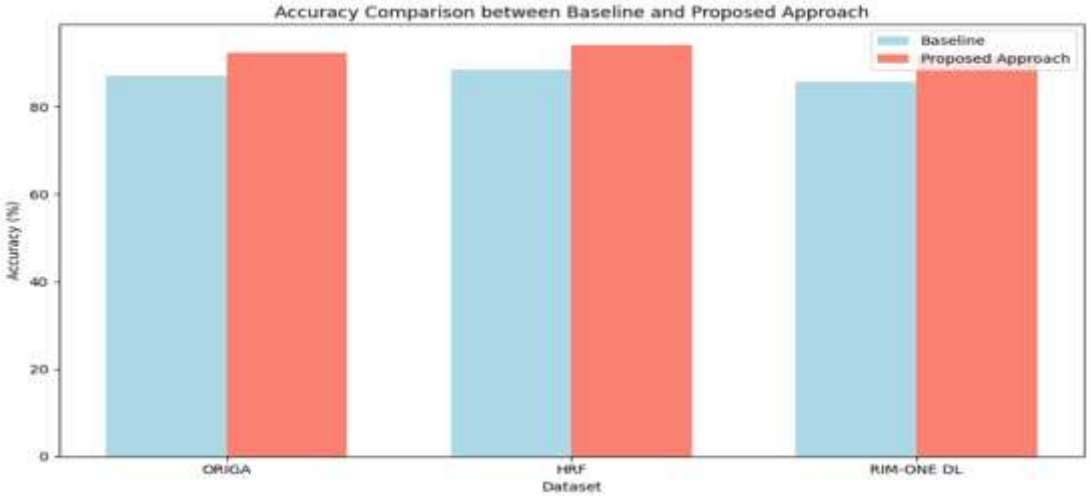

Fig. 4 Accuracy Comparison between Baseline and Proposed Model.

Fig 4 describe the two comparative bar charts illustrate the effectiveness of the proposed glaucoma detection model in relation to the baseline approach across three benchmark datasets: ORIGA, HRF, and RIM-ONE DL. The first chart, focused on accuracy, demonstrates a consistent improvement in classification performance using the proposed model. Indeed, the proposed model obtains accuracies of 92.5%, 94.1%, and 91.7% on ORIGA, HRF, and RIM-ONE DL, respectively, giving it an edge over the baseline model, which scored 87.2%, 88.5%, and 85.7% on the same datasets. This enhancement shows that with some improvements including multi-modal feature extraction, optimized preprocessing, and the incorporation of U-Net and Grad-CAM, the model gets better at distinguishing between glaucomatous and healthy fundus images.

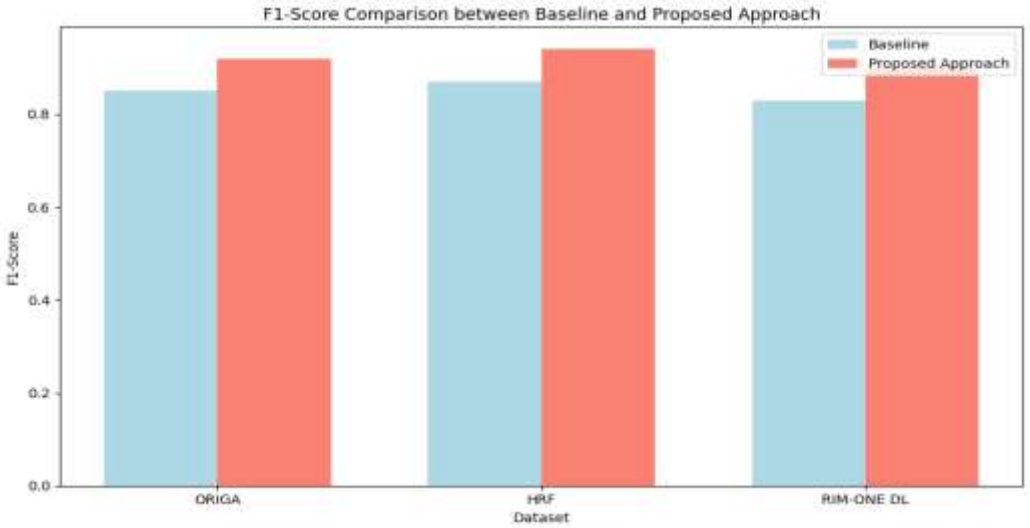

Figure 5: F1-Score Comparison between Baseline and Proposed Approach across Datasets

The figure 5 presents a comparison of F1-scores, which mean a product of harmonic mean of recall and precision. Whereas these scores were 0.92, 0.94, and 0.90 for ORIGA, HRF, and RIM-ONE DL datasets, respectively, and thus established the stronger performance of the proposed model, the baseline, on the other hand, got corresponding F1-scores of 0.85, 0.87, and 0.83 for the same datasets. This enhancement is, however, crucial from the perspective of medical diagnostics, where a low false-negative rate is the key concern. Conversely, these relatively higher F1-scores indicate that better performance by the proposed model should also be evidenced in clinical scenarios where both sensitivity and specificity are required, in addition to gross accuracy. From a generalized view, the evidences stand that the suggested changes have greatly enhanced the model efficiency in detecting glaucoma.

VI. CONCLUSION:

The enhanced glaucoma detection framework successfully overcomes the limitations of the baseline EfficientDet-D0 model by integrating multimodal feature extraction, U-Net segmentation, XAI techniques, and model optimization strategies, resulting in improved accuracy, better segmentation performance, and greater clinical interpretability. Through experiments conducted on ORIGA, HRF, and RIM-ONE DL datasets, the system demonstrated strong generalization and the ability to detect even early glaucomatous changes with high reliability. The significant improvements in accuracy, F1-score, and IoU validate the effectiveness of the proposed enhancements in distinguishing glaucomatous from healthy retinal images. Moreover, the incorporation of pruning, quantization, and distillation minimizes computational cost, making the model suitable for low-resource clinical environments where early detection is essential but advanced hardware is not always available. Overall, this study provides a clinically meaningful, efficient, and explainable solution for large-scale glaucoma screening.

VII. References:

[1] Ling, H. W. (2022). Is glaucoma a local or systemic disease?. EC Ophthalmology, 13, 17-27.

[2] Sarsam, S. M., & Al-Samarraie, H. (2022). Early-stage detection of eye diseases on microblogs: glaucoma recognition. International Journal of Information Technology, 14(1), 255-264. https://doi.org/10.1007/s41870-021-00726-7

[3] Abdullah, F., Imtiaz, R., Madni, H. A., Khan, H. A., Khan, T. M., Khan, M. A., & Naqvi, S. S. (2021). A review on glaucoma disease detection using computerized techniques. IEEE Access, 9, 37311-37333.

[4] Alawad, M., Aljouie, A., Alamri, S., Alghamdi, M., Alabdulkader, B., Alkanhal, N., & Almazroa, A. (2022). Machine learning and deep learning techniques for optic disc and cup segmentation–a review. Clinical Ophthalmology, 747-764. https://doi.org/10.2147/OPTH.S348479

[5] Machiele, R., Motlagh, M., Zeppieri, M., & Patel, B. C. (2024). Intraocular pressure. In StatPearls [Internet]. StatPearls Publishing.

[6] Chauhan, B. C., Vianna, J. R., Sharpe, G. P., Demirel, S., Girkin, C. A., Mardin, C. Y., ... & Burgoyne, C. F. (2020). Differential effects of aging in the macular retinal layers, neuroretinal rim, and peripapillary retinal nerve fiber layer. Ophthalmology, 127(2), 177-185. doi:10.1016/j.ophtha.2019.09.013.

[7] Jammal, A. A., Thompson, A. C., Mariottoni, E. B., Estrela, T., Shigueoka, L. S., Berchuck, S. I., & Medeiros, F. A. (2021). Impact of intraocular pressure control on rates of retinal nerve fiber layer loss in a large clinical population. Ophthalmology, 128(1), 48-57. doi:10.1016/j.ophtha.2020.06.027.

[8] Tonti, E., Tonti, S., Mancini, F., Bonini, C., Spadea, L., D'Esposito, F., ... & Zeppieri, M. (2024). Artificial intelligence and advanced technology in glaucoma: A review. Journal of Personalized Medicine, 14(10), 1062.

[9] Musa, I., Bansal, S., & Kaleem, M. A. (2022). Barriers to care in the treatment of glaucoma: socioeconomic elements that impact the diagnosis, treatment, and outcomes in glaucoma patients. Current Ophthalmology Reports, 10(3), 85-90. https://doi.org/10.1007/s40135-022-00292-6

[10] Fujita, H. (2020). AI-based computer-aided diagnosis (AI-CAD): the latest review to read first. Radiological physics and technology, 13(1), 6-19. https://doi.org/10.1007/s12194-019-00552-4

[11] Guergueb, T., & Akhloufi, M. A. (2023). A review of deep learning techniques for glaucoma detection. SN Computer Science, 4(3), 274. https://doi.org/10.1007/s42979-023-01734-z

[12] Mohammadjafari, A., Lin, M., & Shi, M. (2025). Deep Learning-Based Glaucoma Detection Using Clinical Notes: A Comparative Study of Long Short-Term Memory and Convolutional Neural Network Models. Diagnostics, 15(7), 807. https://doi.org/10.3390/diagnostics15070807

[13] Hasan, M.M., Phu, J., Wang, H. et al. OCT-based diagnosis of glaucoma and glaucoma stages using explainable machine learning. Sci Rep 15, 3592 (2025). https://doi.org/10.1038/s41598-025-87219-w

[14] Kovalyk-Borodyak, O., Morales-Sánchez, J., Verdú-Monedero, R., & Sancho-Gómez, J. L. (2025). Glaucoma detection: Binocular approach and clinical data in machine learning. Artificial Intelligence in Medicine, 160, 103050. https://doi.org/10.1016/j.artmed.2024.103050

[15] Sivakumar, R., & Penkova, A. (2025). Enhancing glaucoma detection through multi-modal integration of retinal images and clinical biomarkers. Engineering Applications of Artificial Intelligence, 143, 110010. https://doi.org/10.1016/j.engappai.2025.110010

[16] Makala, B. P., & Kumar, D. M. (2025). An Efficiet Glaucoma Prediction and Classification Integrating Retinal Fundus Images and Clinical Data Using Dncnn with Machine Learning Algorithms. Results in Engineering, 104220. https://doi.org/10.1016/j.rineng.2025.104220

[17] Hesham, M., Kareem, G., & Hadhoud, M. (2025). Enhanced real-time glaucoma diagnosis: dual deep learning approach. Bulletin of Electrical Engineering and Informatics, 14(3), 1846-1857. https://doi.org/10.11591/eei.v14i3.8495

[18] Sangchocanonta, S., Pooprasert, P., Lerthirunvibul, N., Patchimnan, K., Phienphanich, P., Munthuli, A., ... & Tantibundhit, C. (2025). Optimizing deep learning models for glaucoma screening with vision transformers for resource efficiency and the pie augmentation method. PloS one, 20(3), e0314111. https://doi.org/10.1371/journal.pone.0314111

[19] Mahmood, M.T., Ucan, O.N. Data and image processing for intelligent glaucoma detection and optic disc segmentation using deep convolutional neural network architecture. Discov Computing 28, 73 (2025). https://doi.org/10.1007/s10791-025-09587-1

[20] Yang, AS., Wang, HS., Li, TJ. et al. Diagnosis of early glaucoma likely combined with high myopia by integrating OCT thickness map and standard automated and Pulsar perimetries. Sci Rep 15, 13614 (2025). https://doi.org/10.1038/s41598-025-97883-7

[21] Ruby Elizabeth, J., Kesavaraja, D., & Juliet, S. E. (2025). A deep learning model based glaucoma detection using retinal images. Journal of Intelligent & Fuzzy Systems, 48(6), 823-834. https://doi.org/10.3233/JIFS-234131

[22] Bajwa, M.N., Malik, M.I., Siddiqui, S.A. et al. Two-stage framework for optic disc localization and glaucoma classification in retinal fundus images using deep learning. BMC Med Inform Decis Mak 19, 136 (2019). https://doi.org/10.1186/s12911-019-0842-8

[23] Jain, A., & Sakalle, V. (2024). A Review of Glaucoma Optic Disk Localization and Classification Machine Learning and Deep Learning Models. International Journal of Innovative Research in Technology and Science, 12(2), 163-176. https://ijirts.org/index.php/ijirts/article/view/25

[24] Sheraz, H., Shehryar, T. & Khan, Z.A. Two stage-network: Automatic localization of Optic Disc (OD) and classification of glaucoma in fundus images using deep learning techniques. Multimed Tools Appl 84, 12949–12977 (2025). https://doi.org/10.1007/s11042-024-19338-x

[25] Ma, X., Cao, G., & Chen, Y. (2024). A review of optic disc and optic cup segmentation based on fundus images. IET Image Processing, 18(10), 2521-2539. https://doi.org/10.1049/ipr2.13115

[26] Balla, G., Hashmi, M. F., & Kotambkar, D. M. (2024). Selective Routing Based Optic Disc Segmentation for Glaucoma Diagnosis. IEEE Sensors Letters. https://doi.org/10.1109/LSENS.2024.3384679

[27] Neelagar, M. B., Manjunath, T. C., Patra, R. K., Jagadish, S., & Mazumder, D. (2024, February). Convolutional Neural Network Based Glaucoma Detection and Classification using Optic Disc Localization. In 2024 International Conference on Integrated Circuits and Communication Systems (ICICACS) (pp. 1-5). IEEE. https://doi.org/10.1109/ICICACS60521.2024.10498855

[28] Chen Y, Bai Y, Zhang Y. 2024. Optic disc and cup segmentation for glaucoma detection using Attention U-Net incorporating residual mechanism. PeerJ Computer Science 10:e1941 https://doi.org/10.7717/peerj-cs.1941

[29] Sanghavi, J., & Kurhekar, M. (2024). An efficient framework for optic disk segmentation and classification of Glaucoma on fundus images. Biomedical Signal Processing and Control, 89, 105770. https://doi.org/10.1016/j.bspc.2023.105770

[30] Subha, V., Rayen, S. N. P., & Boopathi, M. (2024). Machine Learning Techniques for Glaucoma Screening Using Optic Disc Detection. Computational Intelligence: Theory and Applications, 321-347. https://doi.org/10.1002/9781394214259.ch15